case for such variations in phosphorus–carbon bond lengths but we wish to draw attention to the possibility.

Acknowledgment. We thank the National Research Council of Canada and the University of Alberta for their financial support.

Registry No. $RhCl(P(C_6H_5)_3)_3$, 14694-95-2.

Supplementary Material Available: Listings of structure factor amplitudes (7 pages). Ordering information is given on any current masthead page.

References and Notes

(1) M. A. Bennett and P. A. Longstaff, *Chem. Ind. (London)*, 846 (1965).
(2) J. F. Young, J. A. Osborne, F. H. Jardine, and G. Wilkinson, *Chem. Commun.*, 131 (1965).
(3) P. B. Hitchcock, M. McPartlin, and R. Mason, *Chem. Commun.*, 1367 (1969).
(4) Footnote *e*, Table III in ref 20.
(5) Personal communication from R. Mason, University of Sussex, Sussex, England.
(6) M. J. Bennett and P. B. Donaldson, *J. Am. Chem. Soc.*, **93**, 3307 (1971).
(7) M. J. Bennett and P. B. Donaldson, submitted for publication in *Inorg. Chem.*
(8) Microanalysis performed by Pascher Microanalytisches Laboratorium, Bonn, West Germany.
(9) P. W. Corfield, R. J. Doedens, and J. A. Ibers, *Inorg. Chem.*, **6**, 197 (1967).
(10) Analysis performed at the University of Alberta.
(11) D. Cromer and J. Mann, *Acta Crystallogr., Sect. A*, **24**, 321 (1968).
(12) R. Mason and G. B. Robertson, *Adv. Struct. Res. Diffr. Methods*, **2**, 57 (1966).
(13) "International Tables for X-Ray Crystallography", Vol. III, Kynoch Press, Birmingham, England, 1962.
(14) W. C. Hamilton, *Acta Crystallogr.*, **18**, 502 (1965).
(15) C. T. Prewitt, Ph.D. Thesis, Massachusetts Institute of Technology, 1963, p 163.
(16) W. C. Hamilton, Brookhaven National Laboratory, Upton, N.Y.
(17) W. Busing and H. A. Levy, Report ORNL-TM-306, Oak Ridge National Laboratory, Oak Ridge, Tenn., 1964.
(18) A. Zalkin, University of California; modified by B. Foxman.
(19) C. K. Johnson, Report ORNL-3794, Oak Ridge National Laboratory, Oak Ridge, Tenn., 1965.
(20) T. Napier, D. W. Meek, R. M. Kirchnev, and J. A. Ibers, *J. Am. Chem. Soc.*, **95**, 4194 (1973).
(21) M. J. Bennett, P. B. Donaldson, P. B. Hitchcock, and R. Mason, *Inorg. Chim. Acta*, **12**, L9 (1975).
(22) W. D. Horrocks, Jr., and R. C. Taylor, *Inorg. Chem.*, **2**, 723 (1963).
(23) R. Mason and A. D. C. Towl, *J. Chem. Soc. A*, 1601 (1970).
(24) J. J. Daly, *J. Chem. Soc.*, 3799 (1964).

Contribution from the Laboratoire de Chimie Minérale A, Equipe associée au C.N.R.S. No. 472, 38, Bd Michelet, 44037 Nantes, Cédex, France

Alkali Metal Intercalates of Ta_2S_2C

R. BREC, J. RITSMA, G. OUVRARD, and J. ROUXEL*

Received June 7, 1976 AIC60413I

Alkali metals were intercalated in the layered structures of Ta_2S_2C. Only first-stage $M_xTa_2S_2C$ phases have been obtained, in which the alkali metals occupy statistically all van der Waals gaps. In the case of potassium, rubidium, and cesium, the alkali metal has a trigonal prismatic coordination, whereas it is octahedrally surrounded for lithium derivatives. The Na–Ta_2S_2C system is a borderline case, with both coordinations for the sodium. The phases, limits, and variation of parameters are given and compared with the results obtained with the TS_2 intercalates. Structures of the $M_xTa_2S_2C$ phases are proposed.

Introduction

The compound Ta_2S_2C prepared by Beckmann, Boller, and Nowotny[1] belongs to the class of the layer chalcogenides. The structure can be regarded as the result of stacking of two-dimensional slabs upon one another along the *c* axis. These slabs are made up of five-layer units, the stacking sequence being S–Ta–C–Ta–S; the heart of a slab consists of a carbon layer and the two external layers are sulfur layers. 1s and 3R forms are known, with octahedral voids in the van der Waals gap (Figure 1).

As in TaS_2 (Figure 1), very weak bonds exist between adjacent layers (van der Waals gap). Therefore, it is expected that various chemical intercalations can pull the layers apart. Boller and Sobczak[2] were able to prepare some ternary compounds $Me_xTa_2S_2C$ (with Me = Ti, V, Cr, ...) whereas some molecular intercalate species were obtained by Schöllhorn and Weiss.[3] In a short note,[4] we have previously shown alkali metal intercalation to occur in Ta_2S_2C. In the present work, a complete survey of the experimental results and of the structures of the derivatives is given.

Experimental Section

Ta_2S_2C was prepared as previously reported by Beckmann et al.[1] Tantalum powder (99.7%), sulfur powder (≥99.99%), and graphite powder (99.999%) were from Koch Light Laboratories. The following sequences also lead to well-crystallized samples; the stoichiometric quantity corresponding to Ta_2S_2C is heated in a sealed silica tube under vacuum for 3 days at 550 °C, then, after returning to room temperature, the product is ground, pelleted, and heated under vacuum up to 1050 °C for 4 days.

The furnace is allowed to cool down again and the product is ground again, pelleted, and finally placed in a carbon tube itself put in a sealed silica tube under vacuum. The sample is then fired at 1200 °C for 2 days and slowly cooled (40 °C/h).

Chunks of pure alkali metal were carefully weighed under nitrogen or argon atmosphere and sealed under vacuum in small breakable ampules. Alkali metals to be intercalated in Ta_2S_2C were dissolved in liquid ammonia. Very dry ammonia was obtained by vacuum distillation from sodium.

The intercalation was performed at room temperature in sealed Pyrex tubes (Figure 2). The tube has two branches, one to separate liquid ammonia from the intercalated powder, and the other containing a thin-walled Pyrex needle to prepare samples for x-ray powder spectra. These precautions had to be taken due to the extreme reactivity of the intercalates toward water and oxygen. Figure 2 helps in the understanding of the way intercalation was performed. A weighed amount of powdered Ta_2S_2C is placed in A, along with a small, breakable ampule containing a determined amount of alkali metal. Pure and dry ammonia is condense frozen and the tube is sealed and brought slowly to room temperature. By shaking the Pyrex tube, the ampule breaks open and intercalation takes place within a minute, with instant decoloration for all $M_xTa_2S_2C$ compositions ($x \leq 1$). Liquid ammonia is then poured into C and frozen. While C is maintained at −180 °C, the intercalation product is heated for 12 h at 250 °C to remove ammonia. To get rid of it, a sealing is made at R_1 and the alkali metal present in it in very small amounts is analyzed to determine the exact amount of the intercalated metal.

The powder of the intercalated compound is stacked in the capillary contained in the remaining Pyrex branch which is sealed in R_2 and opened between R_2 and R_3, the capillary being finally sealed at R_3. Such a system allowed us to get better samples, free of any oxidation.

The intercalation products were carefully reacted with hydrochloric acid, then the aqueous solution was neutralized by NaOH and the Kjeldahl method was used to check that the sample did not contain ammonia. Alkali metal contained in liquid NH_3 was analyzed by flame absorption on a Unicam SP 1900 spectrophotometer.

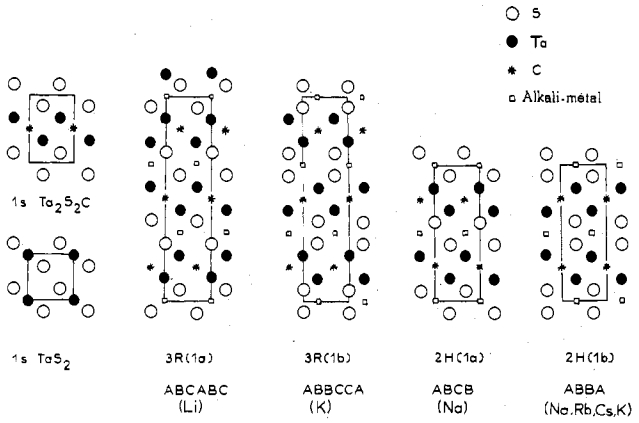

Figure 1. Structural types presented by the $A_xTa_2S_2C$ phases.

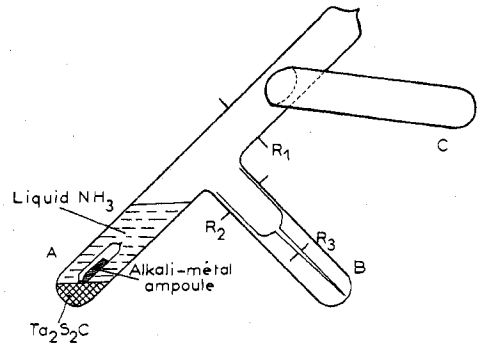

Figure 2. Thick-walled Pyrex tube used to prepare intercalated compounds.

Table I. General Results about $M_xTa_2S_2C$ Phases, with n the Number of Slabs

	Type	Compd	C, Å	n	C/n, Å	a, Å	V, Å^3
	1s	Ta_2S_2C	8.537	1	8.537	3.265	78.81
	3s		25.62	3	8.540	3.276	236.96
Li	3R (Ia)	$Li_1Ta_2S_2C$	26.63	3	8.877	3.302	251.45
Na	2H (Ib)	$Na_{0.15}Ta_2S_2C$	19.50	2	9.75	3.270	180.58
		$Na_{0.80}Ta_2S_2C$	19.35		9.67	3.302	182.71
	2H (Ia)	$Na_{0.85}Ta_2S_2C$	19.30	2	9.65	3.327	185.01
		$Na_1Ta_2S_2C$	19.35		9.67	3.330	185.82
K	3R (Ib)	$K_{0.12}Ta_2S_2C$	31.56	3	10.52	3.265	291.36
		$K_{0.86}Ta_2S_2C$	31.05		10.35	3.299	292.66
Rb	2H (Ib)	$Rb_{0.30}Ta_2S_2C$	21.90	2	10.95	3.280	204.04
		$Rb_{0.84}Ta_2S_2C$	21.45		10.72	3.320	204.75
Cs	2H (Ib)	$Cs_{0.37}Ta_2S_2C$	22.68	2	11.34	3.285	211.96
		$Cs_{0.70}Ta_2S_2C$	22.17		11.08	3.315	210.99

$M_xTa_2S_2C$ phases were studied by x-ray diffraction by means of a Debye–Scherrer camera (Philips PW-1024/10) with a nominal diameter of 114.83 mm. The samples were placed in thin-walled capillaries of 2 mm inner diameter. Cu Kα radiation was used. The a and c parameters were refined by the least-squares method. Tables III to VIII give, along with the spectra, the values of a and c parameters obtained for some compositions of the $M_xTa_2S_2C$ phases. The standard deviations of the parameters are given. To draw the variation of parameters vs. composition, systematic standard errors are taken equal respectively to 0.005 Å for a and 0.05 Å for c.

The limits of the $M_xTa_2S_2C$ phases have been obtained by plotting a and c (parameters of the hexagonal cell) vs. x (alkali metal content). In effect, the structures of the $A_xTa_2S_2C$ phases are closely related to the host structure; the a parameter is slightly changed and the diffraction patterns can be indexed either in a 3R or a 2H form.

Results and Discussion

$A_xTa_2S_2C$ phases have been obtained with $0 \leq x \leq 1$ and A = Li, Na, K, Rb, Cs.

The cell dimensions and cell volumes are collected in Table I for the compositions corresponding to the limits of the various phases. The phase boundaries were obtained by plotting the parameters of evolution vs. composition.

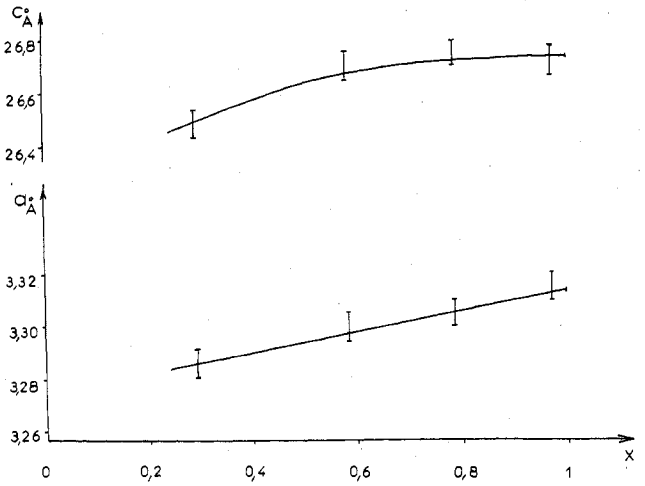

Figure 3. $Li_xTa_2S_2C$: variation of parameters vs. x.

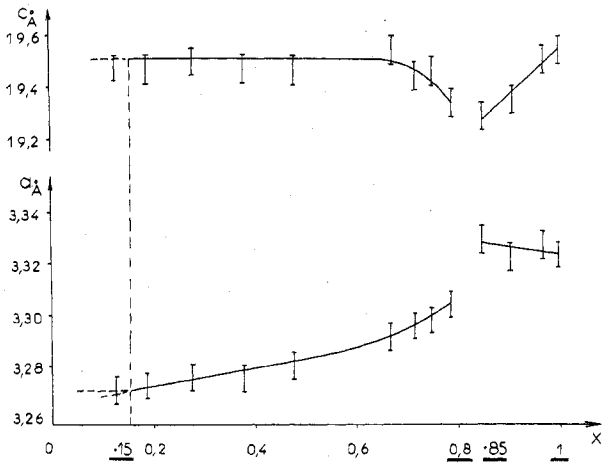

Figure 4. $Na_xTa_2S_2C$: variations of parameters vs. x for Ia and Ib phases.

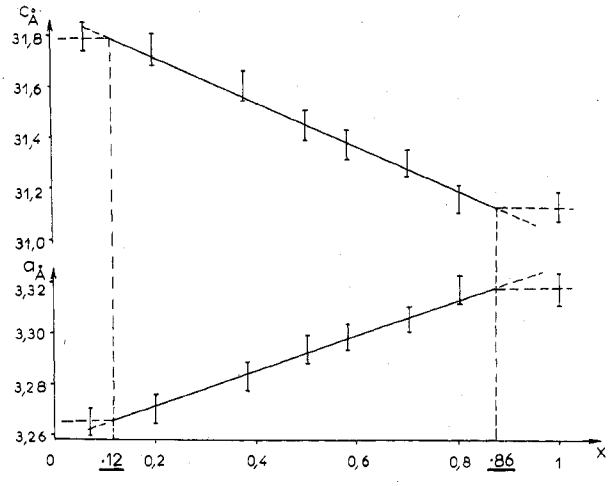

Figure 5. $K_xTa_2S_2C$: variation of parameters vs. x.

In the case of $Li_xTa_2S_2C$, a simple phase is observed with an upper boundary corresponding to $x = 1$. The lower boundary is difficult to ascertain because the parameters tend to those of Ta_2S_2C when x decreases. For the smallest lithium contents, the c parameter expansion is small and a two-phase domain is difficult to observe. The lower limit is in any case smaller than $x = 0.30$ (Figure 3).

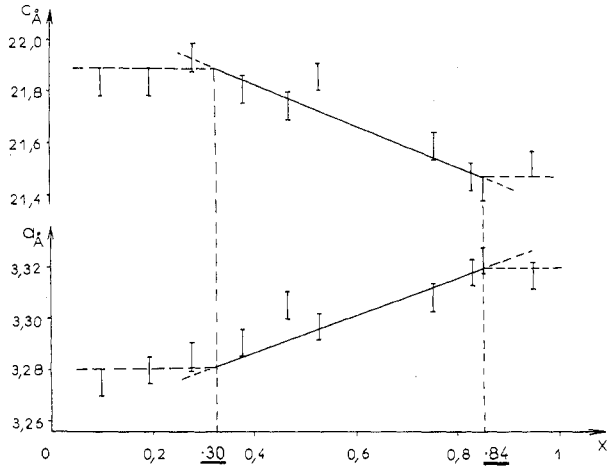

Figure 6. $Rb_xTa_2S_2C$: variation of parameters vs. x.

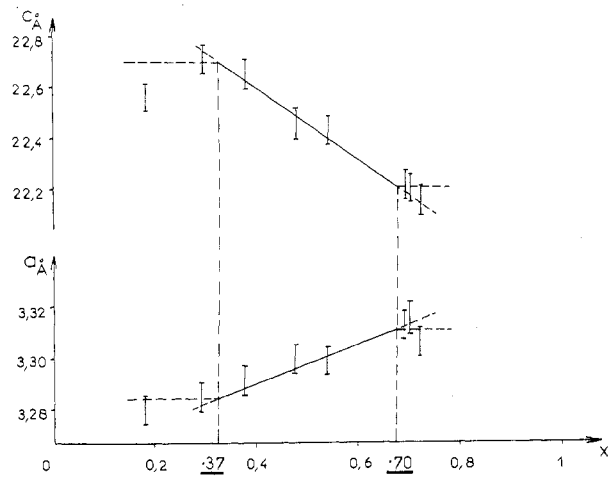

Figure 7. $Cs_xTa_2S_2C$: variation of parameters vs. x.

In the Na–Ta_2S_2C system, two phases, made evident by the drastic change of parameter values from one domain to the other, were observed. The limits are respectively $0.10 \leq x \leq 0.78$ and $0.82 \leq x \leq 1$ (Figure 4).

$K_xTa_2S_2C$ samples are obtained with $0.12 \leq x \leq 0.86$. The c parameter decreases continuously within these limits (Figure 5).

Each of the Rb- and Cs–Ta_2S_2C systems is single phased, with the corresponding limits $0.30 \leq x \leq 0.84$ for Rb and $0.35 \leq x \leq 0.70$ for Cs (Figures 6 and 7).

For all these results (and due to the difficulties of the experimental work), the error affecting x is taken equal to 0.05.

Structural Features of the Intercalated Compounds

Intercalation produces an expansion of the c parameter of the basic Ta_2S_2C structure, while the a axis is only slightly changed. This is considered for the alkali metal to be situated between the Ta_2S_2C slabs. The same behavior has been observed for various intercalates of lamellar disulfides. For the same alkali metal content the observed Δc are gathered in Table II and compared to the values obtained for the corresponding M_xTS_2 phases. Although the M_xTaS_2 and M_xNbS_2 phases correspond to a trigonally surrounded transition metal, the observed Δc appear to be in the range of values we could expect.

The structural studies of A_xNbS_2, A_xTaS_2,[6] A_xTiS_2, A_xZrS_2,[7] and Na_xVS_2[8,9] show the alkali metal coordination to be either octahedral or trigonal prismatic. An extensive study was performed by Rouxel[10] in the case of A_xTiS_2 and A_xZrS_2 phases to determine the various factors affecting structure and chemical bonding in these compounds.

Table II. Change in the c Parameter with Respect to the c Value of the Host Lattice Δc, Å

	T in octahedral coordination			T in trigonal prismatic coordination	
M	$M_{0.65}$-ZrS_2	$M_{0.65}$-TiS_2	$M_{0.65}$-Ta_2CS_2	$M_{0.65}$-NbS_2	$M_{0.65}$-TaS_2
Li	0.37[a]	0.43[a]	0.35[a]	0.51[a]	0.40[a]
Na		1.27[b]	1.21[b]	1.32[a]	1.22[a]
K	1.90[b]	2.01[b]	1.83[b]	2.17[a]	2.05[b]
Rb	2.24[b]	2.48[b]	2.27[b]		
Cs	2.78[b]	2.81[b]	2.58[b]		

[a] (Ia) Octahedral surrounding of the alkali metal (α form).
[b] (Ib) Trigonal prismatic surrounding of the alkali metal (ζ form).

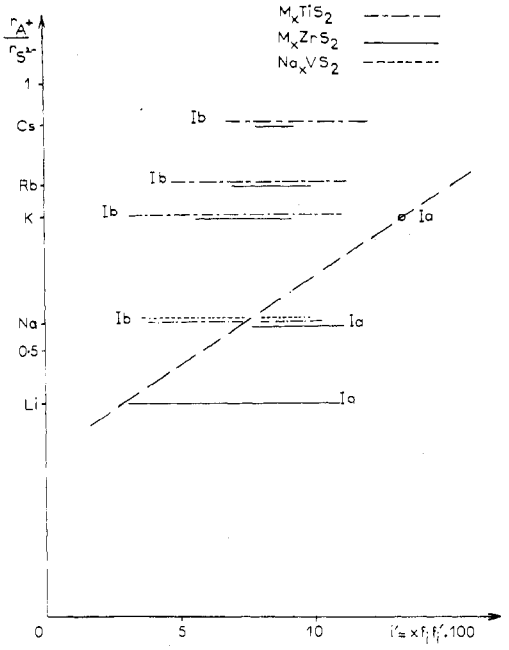

Figure 8. Ionicity–structure diagram for the M_xTS_2 phases.

It has been shown that sulfur surrounding of the alkali metal is related to three factors: the size and the amount of intercalated atoms and the nature of the T–S bond within the slabs of the TS_2 host structure. A general diagram taking into account these three factors has been drawn by plotting the $r_{A^+}/r_{S^{2-}}$ ratio vs. an expression $i' = xf_if'_i$, where x is the amount of the intercalated alkali metal, f_i and f'_i being respectively the fractional ionicities of the A–S and T–S bonds. An unambiguous limit is observed between octahedral (Ia) and trigonal prismatic (Ib) species (Figure 8). This limit fits in well with Wiegers' Na_xVS_2 phases.[8]

In an attempt to expand the diagram to the $A_xTa_2S_2C$ phases, we used the fractional ionicity of the Ta–S bond: $f_i(\text{Ta–S}) = 1 - \exp(-1/4(\chi_{Ta} - \chi_S)^2)$. It can be seen (Figure 9) that the diagram successfully achieves a separation of the various phases on each side of the frontier previously obtained from the A_xTiS_2 and A_xZrS_2 systems. According to this fact it suggests that lithium is octahedrally surrounded by sulfur, whereas potassium, rubidium, and cesium have a trigonal prismatic coordination. Each of the two $Na_xTa_2S_2C$ phases is thought to belong to one of the two possibilities. Sodium would be a borderline case as in the A_xTiS_2 system and this is consistent with the same value of the electronegativity of Ti and Ta (1.5 in the Pauling electronegativity scale).

Furthermore, the variations of a and c vs. alkali metal content for all the intercalates agree well with the rules previously described for the intercalation compounds according to the structural model:[7] for a trigonal prismatic coordination

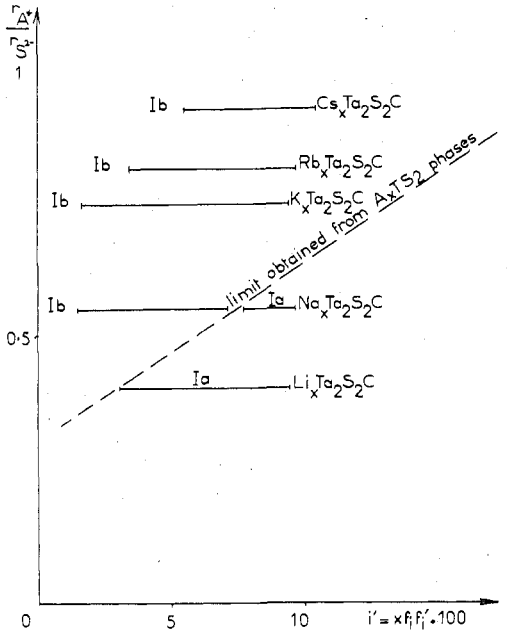

Figure 9. Ionicity–structure diagram applied to the $A_xTa_2S_2C$ phases.

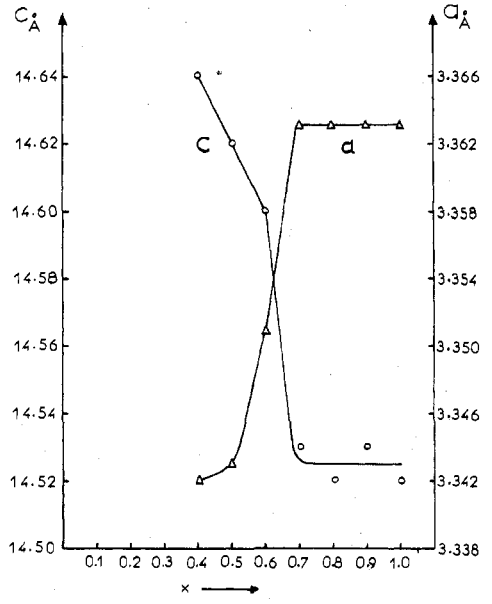

Figure 10. Unit-cell dimensions of the ζ forms of Na_xNbS_2 as a function of the starting composition, after Jellinek.[6]

of the alkali metal the c parameter changes slightly, or decreases (for the bigger alkali metals), with increasing x, whereas the a parameter increases. For an octahedral coordination, c increases with increasing x, whereas a decreases (except for lithium). This rule applies to ξ-Na_xNbS_2 for which the diagram $c = f(x)$ and $a = f(x)$ has been drawn by Jellinek et al. (Figure 10).

In our short note,[4] we had proposed an indexing of the powder spectra based on a 3R cell for all the compounds. Final results show that better agreement is reached in some cases with a 2s cell. As it appears in Table I, $Li_xTa_2S_2C$ has a rhombohedral 3R cell, whereas the two $Na_xTa_2S_2C$ phases, $Rb_xTa_2S_2C$, and $Cs_xTa_2S_2C$ present a 2H cell.

In the case of $K_xTa_2S_2C$, a 2H indexation of the powder spectra leads to a good agreement for the higher values of x. However, for some smaller alkali metal content samples, a 3R indexation gives as good results as the 2H one. In some other cases, a satisfactory indexation is achieved by considering both a 2H and a 3R cell. These facts would suggest either the

Table III. Powder Spectra of 3R(Ia) $Li_{0.58}Ta_2S_2C$ (a = 3.297 (2) Å, c = 26.67 (2) Å)

d_{obsd}	d_{calcd}	hkl	I/I_0
8.90	8.89	003	100
4.46	4.44	006	10
2.966	2.963	009	50
2.831	2.839	101	80
2.623	2.625	104	50
2.513	2.517	015	50
2.224	2.222	0,0,12	50
1.778	1.778	0,0,15	30
1.649	1.649	110	80
1.619	1.621	113	50
1.537	1.546	116	10
1.440	1.441 1.439	119 1,0,16	30
1.421	1.426	021	30
1.399	1.396	024	30
1.373	1.375	0,1,17	30
1.324	1.324	1,1,12	50
1.272	1.270	0,0,21	30
1.210	1.209	1,1,15	50
1.079	1.078	211	50
1.066	1.065	214	10
1.005	1.006	1,1,21	30
0.9530	0.9518	030	50

Table IV. Powder spectra of 2H(Ib) $Na_{0.75}Ta_2S_2C$ (a = 3.300 (1) Å, c = 19.44 (1) Å)

d_{obsd}	d_{calcd}	hkl	I/I_0
9.71	9.72	002	100
3.24	3.24	006	30
2.855	2.858	010	50
2.816	2.827	011	10
2.605	2.614	013	50
2.438	2.429	008	30
2.300	2.302	015	50
1.983	1.991	017	10
1.945	1.944	0,0,10	30
1.651	1.650	110	80
1.625	1.626	112	50
1.472	1.470	116	30
1.427	1.429	020	30
1.396	1.395	023	50
1.369	1.371	024	30
1.344	1.341	025	50
1.260	1.258	1,1,10	50
1.0790	1.0797 1.0800	0,0,18 120	30
1.0653	1.0653	123	50
1.0418	1.0406	125	50

Table V. Powder Spectra of 2H(Ia) $Na_{0.91}Ta_2S_2C$ (a = 3.320 (1) Å, c = 19.34 (2) Å)

d_{obsd}	d_{calcd}	hkl	I/I_0
9.71	9.67	002	100
3.229	3.223	006	30
2.871	2.875	010	50
2.838	2.843	011	30
2.620	2.625	013	80
2.412	2.417	008	30
2.307	2.307	015	100
2.004	1.992	017	10
1.932	1.934	0,0,10	30
1.660	1.660	110	80
1.633	1.636	112	50
1.475	1.476	116	30
1.431	1.433	021	30
1.401	1.403	023	30
1.3682	1.3683	118	50
1.3470	1.3473	025	50
1.2588	1.2595	1,1,10	50
1.0845	1.0848	121	30
1.0712	1.0714	123	30
1.0468	1.0460	125	50
1.0130	1.0110	127	10
0.9768	0.9770	1,1,16	10

Table VI. Powder Spectra of 3R(Ib) $K_{0.50}Ta_2S_2C$ (a = 3.292 (1) Å, c = 31.24 (2) Å)

d_{obsd}	d_{calcd}	hkl	I/I_0
10.39	10.41	003	80
3.44	3.47	009	10
2.834	2.839	101	10
2.790	2.805	012	30
2.594	2.594	015	50
2.396	2.403	107	50
2.299	2.303	018	50
2.108	2.106	1,0,10	10
2.079	2.083	0,0,15	50
1.757	1.757	0,1,14	10
1.647	1.646	110	100
1.626	1.626	113	80
1.547	1.545	0,1,17	10
1.490	1.487	119	10
1.422	1.420 1.424	202 021	80
1.393	1.391	1,1,12	50
1.360	1.358	027	10
1.341	1.339	208	10
1.303	1.302	0,0,24	10
1.295	1.297	0,2,10	50
1.197	1.194 1.201	1,1,18 2,0,14	10
1.126	1.126	2,0,17	10
1.076	1.075 1.077 1.077	122 0,2,19 211	50
1.062	1.062	125	50
1.048	1.048	217	50
1.042	1.042	0,0,30	30
1.021	1.021	1,1,24	50
0.9507	0.9503	030	50

Table VII. Powder Spectra of 2H(Ib) $Rb_{0.75}Ta_2S_2C$ (a = 3.305 (1) Å, c = 21.60 (2) Å)

d_{obsd}	d_{calcd}	hkl	I/I_0
10.87	10.80	002	100
5.41	5.40	004	10
3.59	3.60	006	30
2.869	2.862	010	50
2.829	2.837	011	50
2.650	2.660	013	50
2.382	2.386	015	80
2.155	2.160	0,0,10	50
2.104	2.099	017	30
1.797	1.800	0,0,12	30
1.653	1.653	110	80
1.632	1.633	112	50
1.499	1.502	116	30
1.431	1.428	021	30
1.405	1.404	023	30
1.358	1.358	025	50
1.311	1.312	1,1,10	50
1.218	1.217	1,1,12	30
1.175	1.172	1,1,13	10
1.081	1.081	121	30
1.069	1.070	123	30
1.049	1.049	125	30
1.021	1.021	127	30

possibility of two $K_xTa_2S_2C$ phases (but no drastic change in the parameter's evolution has been observed) or the occurrence of a 6H phase.

Tables III to VIII give the x-ray powder diffraction data for some $M_xTa_2S_2C$ phases.

Considering the octahedral or trigonal prismatic coordination of the alkali as deduced from the ionicity diagram, and taking into account the two kinds of cells (3R and 2H), we obtained the only possible structures 3R(Ia), 3R(Ib), 2H(Ia) and 2H(Ib).[11]

In order to find the structures of our phases, it was necessary to determine the various possible stackings of the Ta_2S_2C slabs, in relation to the type of cell (3R or 2H) and the surrounding

Table VIII. Powder Spectra of 2H(Ib) $Cs_{0.54}Ta_2S_2C$ (a = 3.297 (1) Å, c = 22.44 (1) Å)

d_{obsd}	d_{calcd}	hkl	I/I_0
11.22	11.22	002	100
5.60	5.61	004	30
3.74	3.74	006	30
2.860	2.855	010	50
2.805	2.805	008	50
2.657	2.667	013	50
2.416	2.409	015	80
2.243	2.244	0,0,10	50
2.138	2.132	017	30
1.864	1.870	0,0,12	30
1.650	1.648	110	80
1.629	1.631	112	50
1.509	1.508	116	30
1.426	1.425	021	50
1.401	1.402 1.402	023 0,0,16	50
1.362	1.360	025	50
1.331	1.328	1,1,10	50
1.308	1.304	027	30
1.238	1.236	1,1,12	30
1.121	1.122	0,0,20	10
1.078	1.079 1.078	120 121	30
1.067	1.068	123	30
1.049	1.049	125	50
0.9950	0.9942	1,1,18	10
0.9506	0.9516	030	50

of the alkali metal. We have considered that the Ta_2S_2C slab structure remains unchanged by the alkali metal intercalation.

Let us consider a 3R stacking, with octahedral voids (3R(Ia)), and let us call A, B, and C the planes of sulfur atoms corresponding to each other by a gliding of ($^1/_3$, $^2/_3$, $^1/_3$) and ($^2/_3$, $^1/_3$, $^2/_3$), implied by the rhombohedral symmetry. We have to combine a six-plane sequence in order to give rise to octahedral sites.

This condition eliminates all but the ABCABC sequence, that is to say:

$$[Me_x]S[TaCTa]S[Me_x]S[TaCTa]S[Me_x]S[TaCTa]S$$
$$\quad A \quad B \quad C \quad A \quad B \quad C$$

This 3R(Ia) structure is the 3R structure of Ta_2S_2C in which the octahedral voids are occupied by the alkali metal (Figure 1). This is the structure occurring for $Li_xTa_2S_2C$. Let us now study the 3R stacking with prismatic voids (3R(Ib)). We readily obtain the very simple following diagram:

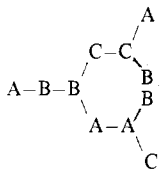

We then keep the only acceptable structure ABBCCA, as the other combinations do not fit in with our rules. We thus obtain the following sequence (Figure 1)

$$[Me_x]S[TaCTa]S[Me_x]S[TaCTa]S[Me_x]S[TaCTa]S$$
$$\quad A \quad B \quad B \quad C \quad C \quad A$$

$K_xTa_2S_2C$ phase could belong to this class.

This 2H(Ia) structure, corresponding to the stacking of four sulfur layers giving rise to octahedral voids, leads to the diagram:

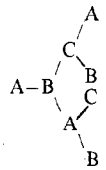

We are left with the only structure which is ABCB (or the equivalent stacking ABAC), the last one, ABAB, does not correspond to a doubling of the c parameter (Figure 1). The structure can be shown by $Na_xTa_2S_2C$ ($0.85 \leq x \leq 1$).

Finally, the 2H(Ib) structure leads very simply to the ABBA stacking. This structure (Figure 1) is the one exhibited by $Rb_xTa_2S_2C$, $Cs_xTa_2S_2C$, and $Na_xTa_2S_2C$ ($0.15 \leq x \leq 0.80$) and possibly by $K_xTa_2S_2C$.

Due to the poor quality of the powder spectra and the weak intensities of the diffraction lines, no structural calculation has been done. Moreover, the hierarchy of the intensities of the spectra for all our compounds remains unchanged which did not allow us to use possible "sensitive" reflections as has been done in previous work about the M_xTS_2 phases.[5]

Conclusion

Nonstoichiometric $A_xTa_2S_2C$ phases have been obtained. They belong to the class of lamellar chalcogenide intercalation compounds. According to the ionicity diagram, the lithium derivative falls within the octahedral domain, potassium, rubidium, and cesium compounds are found to be in the trigonal prismatic region, whereas sodium is a borderline case with both an octahedral and trigonal prismatic phase.

These phases belong to first-stage compounds (all the van der Waals gaps are statistically occupied). No second-stage phase, in which only each alternate gap would be occupied, has been observed; this can be related to the thickness of the Ta_2S_2C slabs separating the A^+ positive layers (screen effect).

Registry No. Ta_2S_2C, 12539-81-0; $LiTa_2S_2C$, 61490-84-4; $NaTa_2S_2C$, 61490-85-5; KTa_2S_2C, 61490-83-3; $RbTa_2S_2C$, 61490-86-6; $CsTa_2S_2C$, 61490-82-2; $Na_{0.75}Ta_2S_2C$, 61490-88-8; $K_{0.50}Ta_2S_2C$, 61490-87-7; $Rb_{0.75}Ta_2S_2C$, 61490-89-9.

References and Notes

(1) O. Beckmann, H. Boller, and H. Nowotny, *Monatsh. Chem.*, **101**, 945, 955 (1970).
(2) H. Boller and R. Sobczak, *Monatsh. Chem.*, **102**, 1226–1233 (1971).
(3) R. Schöllhorn and A. Weiss, *Z. Naturforsch., B*, **28**, 716–720 (1973).
(4) R. Brec, J. Ritsma, G. Ouvrard, and J. Rouxel, *C. R. Hebd. Seances Acad. Sci., Ser. C*, **281**, 531–533 (1975).
(5) J. Cousseau, L. Trichet, and J. Rouxel, *Bull. Soc. Chim. Fr.*, 872–878 (1973).
(6) W. P. Omloo and F. Jellinek, *J. Less-Common Met.*, **20**, 121–129 (1970).
(7) A. Leblanc-Soreau, M. Danot, L. Trichet, and J. Rouxel, *Mater. Res. Bull.*, **9**, 191–198 (1974).
(8) G. A. Wiegers, R. Van der Meer, H. Van Herningen, H. J. Kloosterboer, and A. J. A. Alberink, *Mater. Res. Bull.*, **9**, 1261–1266 (1974).
(9) S. Whittingham and F. Gamble, *Mater. Res. Bull.*, **10**, 363–372 (1975).
(10) J. Rouxel, *J. Solid State Chem.*, **17**, 223–229 (1976).
(11) As used in the previous paper, the parenthetical Ia and Ib mean that the compounds belong to the I stage phase class (each van der Waal's gap statistically occupied), whereas a stands for an octahedral and b for a trigonal prismatic coordination for the alkali metal; 3R and 2H mean respectively a rhombohedral cell with three Ta_2S_2C slabs and a hexagonal cell with two Ta_2S_2C slabs.

Contribution from the Institute of Inorganic Chemistry, University of Frankfurt, D-6000 Frankfurt 70, West Germany

Photoelectron Spectra and Molecular Properties. 59.[1] Ionization Energies of Disulfur Dihalides and Isomerization Surfaces $XSSX \rightleftarrows SSX_2$

BAHMAN SOLOUKI[2] and HANS BOCK*

Received June 8, 1976 AIC60422R

Photoelectron spectra of disulfur dihalides XSSX (X = Cl, Br) are reported and assigned in comparison to those of HSSH and the F_2S_2 isomers. CNDO energy surfaces for the isomerization $XSSX \rightleftarrows X_2SS$ (X = F, Cl, H) yield total energy minima close to those for the known geometries of FSSF, F_2SS, ClSSCl, and HSSH. The most probable reaction path calculated for an intramolecular halogen or hydrogen 1,2 shift involves a three-membered ring. Reflecting the nonexistence of thiothionyl chloride, Cl_2SS, and thiothionyl hydride, H_2SS, only the difluoro isomers are separated by a CNDO total energy barrier high enough to rationalize their achieved isolation.

Disulfur difluoride, FSSF, and thiothionyl difluoride, F_2SS, rank among the more curious isomers of few-atom molecules. First reported[3] independently in 1963 and 1964 by Kuczkowski[4] as well as by Seel and co-workers,[3] they not only resemble each other regarding essential structural parameters[4] but even give rise to almost identical photoelectron spectra[5] (Figure 1).

FSSF is thermally less stable and changes slowly into F_2SS,[3] a unique rearrangement considering all the isosteric compounds currently known to exist exclusively in either the ABBA or the A_2BC structure as, e.g., ClSSCl or F_2SO. Extending previous studies,[6] we wish to report photoelectron (PE) spectra of ClSSCl and BrSSBr,[2,7] an attempt to generate the unstable ISSI in the gas phase, and CNDO total energy surfaces[2] for the F_2S_2, Cl_2S_2, and H_2S_2 systems.

Experimental Section

Disulfur Dihalides. Purified[8] ClSSCl in ether solution was allowed to react with stoichiometric amounts of gaseous dry HBr (generated by slowly dropping bromine into tetraline) to yield either ClSSBr or BrSSBr.[9] After distillation under reduced pressure (ClSSBr, bp 37 °C (0.1 mm); BrSSBr, bp 48 °C (0.1 mm)) traces neither of HBr nor of HCl were revealed by the PE spectra.

In analogy to the synthesis of SSO[10] from Cl_2SO and Ag_2S, preparation and characterization of unstable[11] ISSI were attempted by passing ClSSCl over KI in a heated tube connected to the PE spectrometer (see Figure 2). However, no direct evidence for the generation of ISSI could be obtained with ClSSCl pressures ranging from 0.05 to 1 Torr: below 85 °C the PE spectrum of pure ClSSCl was recorded, between 85 and 110 °C increasing amounts of iodine began to show up, and above 110 °C no more ClSSCl could be detected while outside the oven zone a yellow deposit of elemental sulfur formed.

Photoelectron Spectra. The helium I spectra were recorded using Perkin-Elmer PS 16 instruments with 127° electrostatic deflection analyzers and calibrated by Xe and Ar $^2P_{3/2}$ ionizations. A resolution of ~30 meV was achieved.

Calculations. The CNDO/2 calculations for the XSSX and X_2SS systems with X = F, Cl, H were performed at the Hochschul-Rechenzentrum Frankfurt and included $3d_S$ orbitals in the basis set. The results have been checked and improved by subsequent Koopmans corrections based on a second-order perturbation treatment.[12,13] The Koopmans correlation diagram (Figure 3) containing more than 40 PE spectroscopically assigned ionizations of 13 different sulfur compounds supports the assumed reliability of semiempirical calculations for chemically related molecules, yielding the linear regression[2]

$$-\varepsilon_J^{CNDO} = 0.335 + 0.931(IE_n^V) \quad (1)$$

with the standard deviation SE = 0.431.[2]

For the isomerization surface calculations, the CNDO/2 version used has been coupled to a coordinate program[2] developed to au-